Available online at www.sciencedirect.com
SCIENCE DIRECT®

NUCLEAR SCIENCE AND TECHNIQUES

Nuclear Science and Techniques, Vol.17, No.3 (2006) 170–176

An investigation of flow characteristics and critical heat flux in vertical upward round tube

FAN Pu QIU Sui-Zheng* JIA Dou-Nan

(State Key Laboratory of Multiphase Flow in Power Engineering, Xi'an Jiaotong University, Xi'an 710049, China)

Abstract Prediction of critical heat flux (CHF) in annular flow is important for the safety of once-through steam generator and the reactor core under accident conditions. The dryout in annular flow occurs at the point where the film is depleted due to entrainment, deposition, and evaporation. The film thickness, film mass flow rate along axial distribution, and CHF are calculated in vertical upward round tube on the basis of a separated flow model of annular flow. The theoretical CHF values are higher than those derived from experimental data, with error being within 30%.

Key words Annular flow, Critical heat flux, Dryout, Entrainment, Deposition

CLC number TL33

1 Introduction

The term "annular flow" is used to describe the configuration of vapor-liquid flow, in which part of the liquid travels as a film on the wall and the rest is entrained as drops by the vapor core in the center of the channel, as shown in Fig.1. Annular flow is one of the most common flow patterns encountered in a wide range of industrial applications such as nuclear power plants, evaporators, and condensers. Prediction of critical heat flux (CHF) in annular flow is important for the safety of once-through steam generator and reactor core under accident conditions. Due to the existence of the interfacial wave between the vapor core and liquid, droplets are entrained from the liquid film into the vapor core. The distribution of droplets is not uniform, and their size can vary with time and space. Many experiments denote that the amount of droplets located in the center of channel is the least. The entrainment of liquid film by vapor core has an important influence on the mass transfer, momentum transfer, and heat transfer between the liquid film and vapor core.

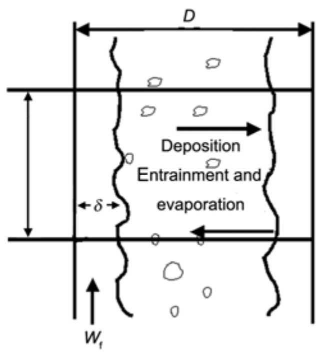

Fig.1 Dryout model of annular flow.

Hewitt [1], Taylor, and Whalley showed that the CHF in annular flow is a dryout of liquid film on the wall according to experiment results. A phenomenological analysis for predicting the dryout heat flux in annular flow was suggested by Isbin and coworkers [2]. Their method was to balance the rates of entrainment and evaporation against the rate of droplet deposition. The result of the approach depends on the accuracy of analytical evaluation of the rate of entrainment and droplet deposition.

In this study, on the basis of liquid film depletion

*E-mail: szqiu@mailst.xjtu.edu.cn
Received date: 2005-12-16

theory, the CHF is predicted and the thickness and the mass flow rate of the liquid film are also calculated along the axial position. At the same time, the influence of certain parameters (such as tube diameter, mass flux, pressure, and the heated length) on the CHF is also analyzed.

2 Analytical model of dryout

2.1 Basic assumptions

To build a reasonable separated flow model of two-phase annular flow, the following assumptions were made:

1) the flow is incompressible;
2) the liquid film thickness is uniform around the periphery;
3) the interface between liquid and vapor is smooth;
4) the pressure is uniform in the radial direction;
5) liquid droplets entrained in the vapor core are uniformly distributed;
6) the flow is steady.

2.2 Liquid film mass conservation equation

The entrainment, deposition of liquid droplets, and evaporation of liquid film will lead to variation in the mass flow rate of liquid film along the axial position. The mass conservation equation of liquid film at position Z of tube is:

$$\mathrm{d}W_{\mathrm{f}}/\mathrm{d}z = p_{\mathrm{r}}(D - E - \frac{q}{h_{\mathrm{fg}}}) \tag{1}$$

where W_{f} is the mass flow rate of liquid film, D and E refer to the deposition rate and entrainment rate of droplet per unit interfacial area, respectively.

2.3 Triangular relationship of annular flow

The triangular relationship of annular flow refers to the inter relationships among liquid film thickness δ, pressure gradient $\mathrm{d}p/\mathrm{d}z$, and the mass flow rate of liquid film W_{f}.

As shown in Fig. 2, all the force acting on the cylindrical liquid film bounded by d_{i} and d of length $\mathrm{d}z$ includes gravitational force, interfacial shear stress τ_i, and shear stress within the liquid film τ. According to the force balance on the annular ring element and ignoring the acceleration, the shear stress τ within the liquid film at radius r is as follows:

$$\tau = \frac{\tau_{\mathrm{i}} r_{\mathrm{i}}}{r} + \frac{1}{2}(\rho_{\mathrm{l}} g + \frac{\mathrm{d}p}{\mathrm{d}z})\frac{(r_{\mathrm{i}}^2 - r^2)}{r} \tag{2}$$

where $\tau_{\mathrm{i}} = \frac{(r_{\mathrm{o}} - \delta)}{2}(-\frac{\mathrm{d}p}{\mathrm{d}z} - \rho_{\mathrm{g}} g)$ and using the concept of eddy viscosity model:

$$\frac{\mathrm{d}u}{\mathrm{d}y} = \frac{\tau}{\mu} = \frac{\tau}{\mu_{\mathrm{l}} + \varepsilon_{\mathrm{m}}\rho_{\mathrm{l}}} \tag{3}$$

Replacing τ in Eq. (3) by Eq. (2), we obtain:

$$\frac{\mathrm{d}u}{\mathrm{d}y} = \frac{\tau_{\mathrm{i}}}{\mu_{\mathrm{l}} + \varepsilon_{\mathrm{m}}\rho_{\mathrm{l}}}\left(\frac{r_{\mathrm{o}} - \delta}{r_{\mathrm{o}} - y}\right) + \frac{1}{2}(\rho_{\mathrm{l}} g + \frac{\mathrm{d}p}{\mathrm{d}z}) \times \left(\frac{r_{\mathrm{o}} - y}{\mu_{\mathrm{l}} + \varepsilon_{\mathrm{m}}\rho_{\mathrm{l}}}\right)\left[\left(\frac{r_{\mathrm{o}} - \delta}{r_{\mathrm{o}} - y}\right)^2 - 1\right] \tag{4}$$

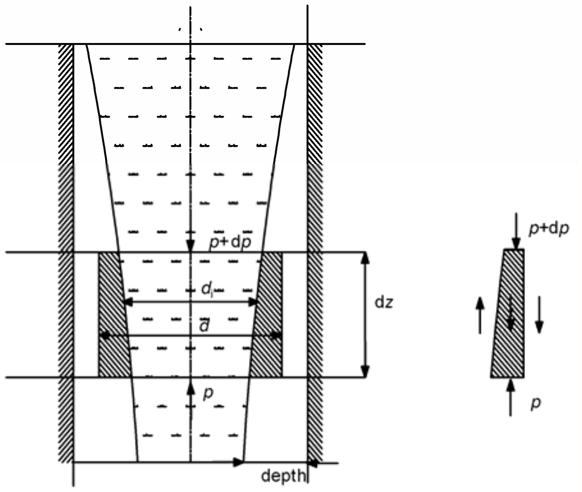

Fig. 2 Force of liquid film in vertical upward annular flow.

The velocity of the liquid film u at radius r can be attained if Eq. (4) is integrated as follows:

$$u = \int_0^r \frac{\mathrm{d}u}{\mathrm{d}y}\mathrm{d}y = \int_0^r \left[\frac{\tau_{\mathrm{i}}}{\mu_{\mathrm{l}} + \varepsilon_{\mathrm{m}}\rho_{\mathrm{l}}}\left(\frac{r_{\mathrm{o}} - \delta}{r_{\mathrm{o}} - y}\right) + \frac{1}{2}(\rho_{\mathrm{l}} g + \frac{\mathrm{d}p}{\mathrm{d}z}) \times \left(\frac{r_{\mathrm{o}} - y}{\mu_{\mathrm{l}} + \varepsilon_{\mathrm{m}}\rho_{\mathrm{l}}}\right)\left[\left(\frac{r_{\mathrm{o}} - \delta}{r_{\mathrm{o}} - y}\right)^2 - 1\right]\right]\mathrm{d}y \tag{5}$$

The mass flow rate of the liquid film W_{f} can be obtained through integrating Eq. (5):

$$W_{\mathrm{f}} = \int_0^{\delta} 2\pi r u \rho_{\mathrm{l}}\,\mathrm{d}y \tag{6}$$

2.4 Pressure gradient $\mathrm{d}p/\mathrm{d}z$ model

Following Hewwit and Hall-Tayor [3], a momentum conservation on the vapor core, which includes momentum exchange due to entrainment, results in:

$$-\frac{\mathrm{d}\,p}{\mathrm{d}\,z}=\{\frac{2\tau_{\mathrm{i}}}{r_{\mathrm{i}}}+\frac{\rho_{\mathrm{g}}g[x+e(1-x)]}{x+e(1-x)\dfrac{\rho_{\mathrm{g}}}{\rho_{\mathrm{l}}}}+\frac{G^2}{\alpha}\times$$

$$\frac{\mathrm{d}}{\mathrm{d}\,z}[\frac{x^2}{\alpha\rho_{\mathrm{g}}}+\frac{(1-e)^2(1-x)^2x}{\rho_l(1-\alpha)-\rho_{\mathrm{g}}e(1-x)}+\frac{e(1-x)x}{\alpha\rho_{\mathrm{g}}}]\} \quad (7)$$

where $\mathrm{d}\,p/\mathrm{d}\,z$ is the pressure gradient along the axial position, and e is the entrainment fraction and is equal to the ratio of mass flow rate of droplets entrained in vapor core to the mass flow rate of the total liquid.

2.5 Deposition rate and entrainment rate

2.5.1 Entrainment rate model

In vertical annular flow, the entrainment takes place when the velocity of the vapor core is high enough to produce interfacial wave. Thus, the liquid is stripped from the wave crest and is entrained into the vapor core. To obtain an analytical solution for annular flow, it is necessary to acquire the entrainment amount from the liquid film. Currently, entrainment fraction of liquid droplet, or entrainment rate, mainly depends on the experimental measurements and empirical correlations. Among these correlations, Ishii and Mishima's correlation [4] is generally accepted. But the correlation can only be applied to the condition of air–water at low pressure. So Okawa *et al*. [5] tried to develop a new entrainment rate correlation for accurately predicting the flow rates of liquid film and droplets in annular-dispersed two-phase flow under a wide range of flow conditions. In their model, the liquid droplet entrainment rate is proportional to the following dimensionless number, π_{E}, which is obtained by dividing the interfacial shear force by the retaining force of surface tension:

$$\pi_{\mathrm{E}}=\frac{f_{\mathrm{i}}\rho_{\mathrm{g}}J_{\mathrm{g}}^2\delta}{\sigma}$$

Many researchers also point out that at equilibrium condition, the entrainment rate will increase with the increasing interfacial shear stress and the decreasing surface tension, which is in accordance with Tomio Okawa's entrainment rate theory.

Kataoka's [6] entrainment rate model is applied in this article:

$$\frac{ED_{\mathrm{e}}}{\mu_{\mathrm{f}}}=0.72\times10^{-9}Re_{\mathrm{f}}^{1.75}We(1-e_\infty)^{0.25}(1-\frac{e}{e_\infty})^2+$$
$$6.6\times10^{-7}(Re_{\mathrm{f}}We)^{0.925}\left(\frac{\mu_{\mathrm{g}}}{\mu_{\mathrm{f}}}\right)^{0.26}(1-e)^{0.185},\quad e\le e_\infty$$
$$\frac{ED_{\mathrm{e}}}{\mu_{\mathrm{f}}}=6.6\times10^{-7}(Re_{\mathrm{f}}We)^{0.925}\left(\frac{\mu_{\mathrm{g}}}{\mu_{\mathrm{f}}}\right)^{0.26}(1-e)^{0.185},e>e_\infty$$
$$E=0,\qquad Re_{\mathrm{f}}<Re_{\mathrm{fc}} \quad (8)$$

where $We=\dfrac{\rho_{\mathrm{g}}j_{\mathrm{g}}^2D_{\mathrm{h}}}{\sigma}\left(\dfrac{\rho_{\mathrm{f}}-\rho_{\mathrm{g}}}{\rho_{\mathrm{g}}}\right)^{1/3}$; $Re_{\mathrm{f}}=\dfrac{\rho_{\mathrm{f}}j_{\mathrm{f}}D_{\mathrm{h}}}{\mu_{\mathrm{f}}}$;

e_∞ is entrainment fraction in Ishii and Mishima's correlation [4]:

$$e_\infty=\mathrm{tgh}(7.25\times10^{-7}We^{1.25}Re_{\mathrm{f}}^{0.25});$$

Re_{fc} is critical Reynolds number:

$$Re_{\mathrm{fc}}=\left(\frac{10}{0.347}\right)^{1.5}\left(\frac{\rho_{\mathrm{l}}}{\rho_{\mathrm{g}}}\right)^{0.75}\left(\frac{\mu_{\mathrm{g}}}{\mu_{\mathrm{f}}}\right)^{1.5}$$

2.5.2 Deposition rate model

Deposition rate is mainly related to the mass transfer coefficient of droplet deposition k and to the droplet concentration in vapor core C:

$$D=kC \quad (9)$$

Considerable theoretical and experimental research have been carried out for the mass transfer of droplet deposition k, and reliable correlations have been developed on the basis of detailed physics analysis of flow structure, vapor core, droplet size, and turbulent diffusion of the droplet. Paleev and Filipovich's correlation [7] for deposition rate is applied in this article:

$$D=kC$$
$$\frac{k}{j_{\mathrm{g}}}=0.022Re_{\mathrm{g}}^{-0.25}\left(\frac{C}{\rho_{\mathrm{f}}}\right)^{-0.26}\left(\frac{\rho_{\mathrm{g}}}{\rho_{\mathrm{f}}}\right)^{0.26}$$
$$C=W_{\mathrm{f}}/[(W_{\mathrm{f}}/\rho_{\mathrm{f}})+(W_{\mathrm{g}}/\rho_{\mathrm{g}})]$$
$$=\rho_{\mathrm{f}}\frac{u_{\mathrm{f}}A_{\mathrm{f}}}{u_{\mathrm{f}}A_{\mathrm{f}}+u_{\mathrm{g}}A_{\mathrm{g}}}=\rho_{\mathrm{f}}\frac{j_{\mathrm{f}}}{j_{\mathrm{f}}+j_{\mathrm{g}}} \quad (10)$$

where $Re_{\mathrm{g}}=j_{\mathrm{g}}D_{\mathrm{h}}/\upsilon_{\mathrm{g}}$.

2.6 Interfacial shear stress model

The interfacial shear stress τ_i in Eq. (7) is one of the most important variables that influences the calculated accuracy of CHF in annular flow, besides the droplet entrainment rate and deposition rate. The correlation proposed by Henstock and Hanratty [8] is used to calculate the interfacial shear stress:

$$\tau_i = \frac{1}{2} f_i \rho_g u_g^2 \tag{11}$$

$$\frac{f_i}{f_s} = 1 + 1400F\left\{1 - \exp\left[-\frac{(1+1400F)^{1.5}}{13.2G_0F}\right]\right\} \tag{12}$$

$$F = \frac{\left[\left(0.707Re_f^{0.5}\right)^{2.5} + \left(0.0379Re_f^{0.9}\right)^{2.5}\right]^{0.4}}{Re_g^{0.9}}\left(\frac{\mu_f}{\mu_g}\right)\left(\frac{\rho_g}{\rho_l}\right)^{0.5} \tag{13}$$

where $u_g = Gx/\rho_g$; $Re_g = GxD_h/\mu_g$; $Re_f = G(1-x)(1-e)D_h/\mu_f$; $f_s = 0.046Re_g^{-0.2}$; $G_0 = D_h g\rho_f/\left(f_s\rho_g u_g^2\right)$.

2.7 Eddy viscosity model

The usual practice in treating the liquid film eddy viscosity of annular flow is to assume that the wall turbulence is similar to that of single-phase flow and to use single-phase flow correlations for the liquid film eddy viscosity. For eddy viscosity ε_m in Eq. (3), the following correlations are applied:

$$\frac{\varepsilon_m}{\upsilon} = 0.001y^{+3} \qquad y^+ < 5$$

$$\varepsilon_m = \left\{Ky\left[1-\exp\left(-\frac{y^+}{25}\right)\right]\right\}^2\left|\frac{du}{dy}\right|\left(1.0-\frac{y}{\delta}\right)^{1.5}\phi, \; y^+ \geq 5 \tag{14}$$

where y^+ is non-dimensional distance, $y^+ = yu^*/\upsilon$; K is Von Karman constant, $K = 0.41$; u^* is non-dimensional frictional velocity, $u^* = \left(\tau_w/\rho_f\right)^{0.5}$; $\phi = B_o^{0.3}\left(\frac{1-x}{x}\right)^{0.1}$; B_o is boiling number, $B_o = q/(Gh_{fg})$.

2.8 Initial mass quality of annular flow

In flow boiling, there exist bubbly flow, slug flow, churn flow, annular flow, and annular-mist flow. For a channel heated by uniform heat flux with some inlet mass quality, the onset of annular flow must be recognized due to the built model in this study that is only applicable to annular flow.

In two-phase flow, the annular flow is assumed to begin when the superficial velocity of the vapor core is greater than the least velocity, which can entrain the emerging largest droplets.

$$j_g \geq \left(\frac{\sigma g(\rho_f - \rho_g)}{\rho_g^2}\right)^{0.25}\left(\frac{\rho_f\sigma}{\sqrt{\sigma/(g(\rho_f-\rho_g))}}\right)^{0.1} \tag{15}$$

The initial mass quality of annular flow is:

$$x = j_g\rho_g/G \tag{16}$$

3 Numerical procedures

3.1 Velocity distribution within liquid film

The velocity distribution within the liquid film can be solved by the integration of Eq. (4). Eq. (4) is a linear equation of du/dy, if the flow is laminar flow. The velocity within the liquid film can be attained directly by the integration of Eq. (4). Otherwise, if the flow is turbulent, Eq. (4) is a quadratic equation of du/dy. In this article, the function Dzreal in International Mathematical Statistical Library (IMSL) is used to solve the quadratic equation.

Integration method of variable step size is applied to solve the velocity of liquid film at some distance y from the wall. First, the integrating range $(0, y)$ is divided into n divisions, du/dy at each node is solved, and u_n at y can be obtained by numerical integration. Subsequently, the integrating range $(0, y)$ is divided into $2n$ divisions, and u_{2n} at y is solved through a similar method. The calculation ends if the error between u_n and u_{2n} is less than ε. Else, the integrating range $(0, y)$ is divided into $4n$ divisions and u_{4n} is attained. Then u_{2n} and u_{4n} are compared until the error between them is less than the set error.

3.2 Flowchart of program procedure

Fig. 3 shows the flowchart of program procedure.

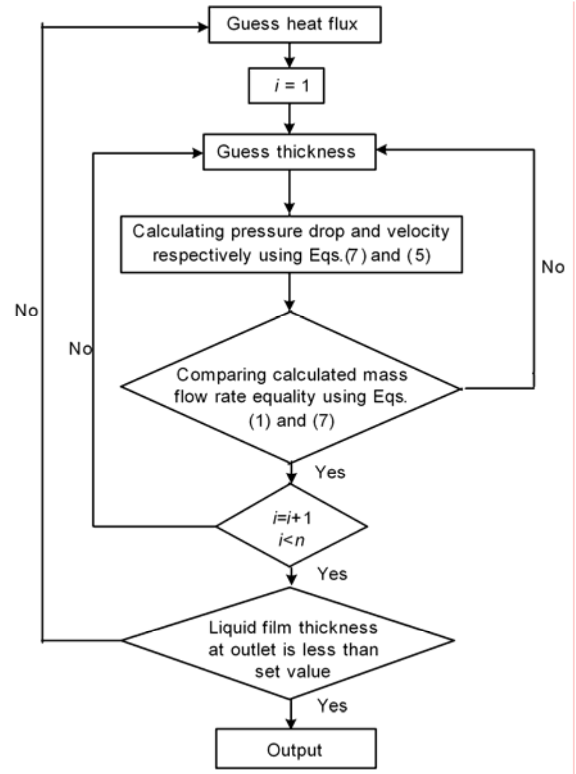

Fig.3 Flowchart of program procedure.

4 Results and analysis

4.1 Calculated results of annular flow

Fig.4 shows the liquid film velocity distribution along a radial direction. The radial velocity at the wall is zero and gradually increases with increasing distance from the wall. Fig. 5 shows the liquid film thickness distribution for different heat fluxes along an axial direction. It can be seen that the thickness of the liquid film is reduced when the heat flux increases, which leads to more intense evaporation. Fig. 6 shows the liquid film thickness distribution for different mass fluxes along an axial direction. The thickness of the liquid film is more when the mass flux is larger. This is attributed to the fact that more liquid is evaporated at less mass flux at the same axial position and same heat flux.

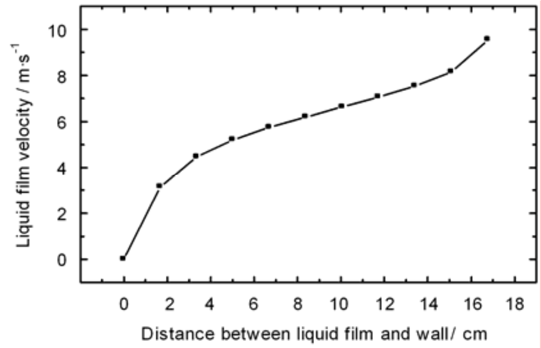

Fig.4 Liquid film velocity distribution along a radial direction.

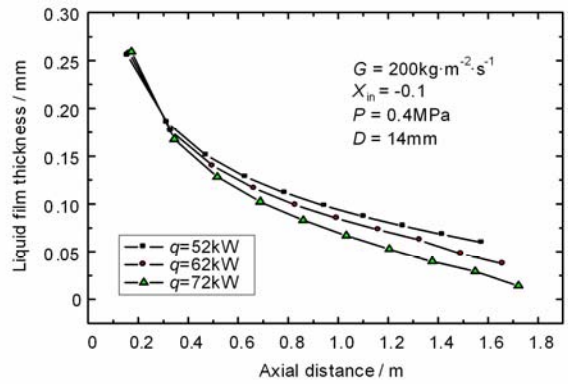

Fig.5 Liquid film thickness distribution for different heat fluxes along an axial direction.

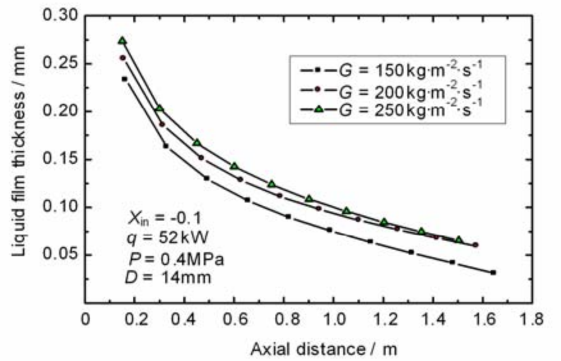

Fig.6 Liquid film thickness distribution for different mass fluxes along an axial direction.

4.2 Calculated results of CHF

In a vertical channel that is heated uniformly, the thickness of the liquid film is reduced gradually due to evaporation, entrainment of droplet, and deposition of droplet, and the mass quality gradually becomes large. Finally, the liquid film is depleted; droplet is entrained in vapor core, and the CHF is reached. In this article, the confirmation of the CHF is through changing the heat flux so that the dryout takes place at the outlet of the channel.

Fig.7 shows the comparison between the calculated results and the experimental results of the study by Ren Ling [9]. The error is within 30%. From Fig.7, it can be seen that the calculated CHF is greater than the experimental CHF, which may be attributed to the fact that the initial entrainment rate at the onset of annular flow is simply treated as zero because of no related theory. At the same time, the entrainment rate correlation should be explained on other grounds.

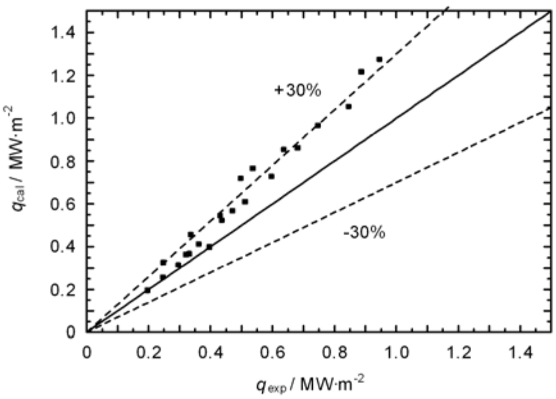

Fig.7 Comparison between calculated results and experimental results.

Fig.8 shows the CHF variation with tube diameter. Fig. 9 shows the CHF variation with inlet mass quality. Fig. 10 shows the CHF variation with mass flux. According to these figures, the CHF increases with increasing tube diameter and increasing mass flux and decreases with increasing inlet mass quality.

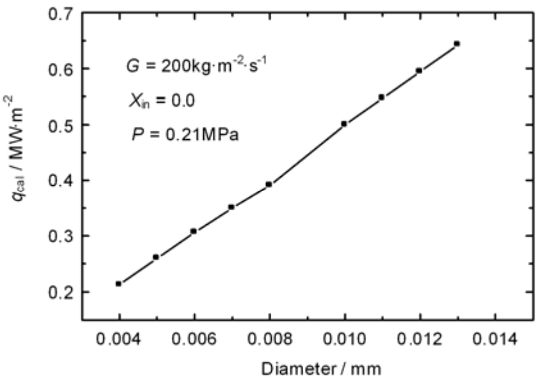

Fig. 8 Critical heat flux variation with tube diameter.

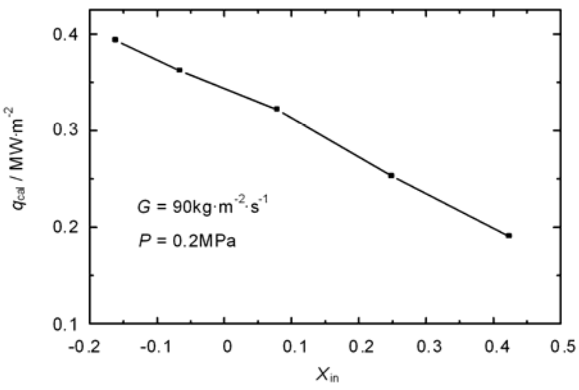

Fig.9 Critical heat flux variation with inlet mass quality.

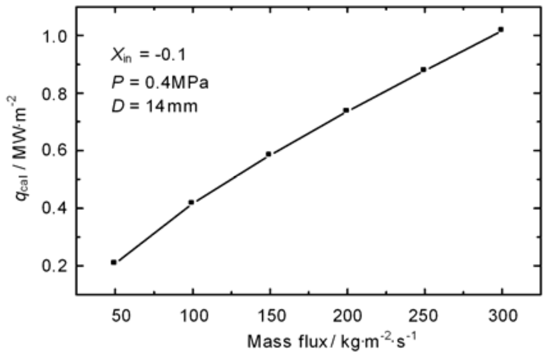

Fig.10 Critical heat flux variation with mass flux.

5 Conclusions

The separated flow model is built to solve CHF in annular flow. On the basis of the theory of liquid film depletion, the film thickness, film mass flow rate distribution along the axial position, and CHF are calculated in vertical upward round tube. The theoretical CHF values are higher than the experimental data, with error being within 30%.

Nomenclature

W_f Mass flow rate of liquid film (kg·s^{-1})
p_r Perimeter of between liquid film and vapor core (m)
q Heat flux (kW·m^{-2})
D Deposition rate of droplet (kg·m^{-2}·s^{-1})
C Droplet concentration in vapor core (kg·m^{-3})
k Mass transfer coefficient (m·s^{-1})
E Droplet entrainment (kg·m^{-2}·s^{-1})
h_{fg} Latent heat of evaporation (kJ·kg^{-1})
τ Shear stress within liquid film at radius r (N·m^{-2})
τ_i Interfacial shear stress (N·m^{-2})
ρ_f Density of liquid phase (kg·m^{-3})

ρ_g Density of vapor (kg·m^{-3})

μ_l Dynamic viscosity of liquid (kg·m^{-1}·s^{-1})

ε_m Eddy viscosity (m^2·s^{-1})

y Distance between liquid film at radius r and wall (m)

r_o Radius (m)

δ Thickness of liquid film (m)

e Entrainment fraction

e_∞ Entrainment fraction at equilibrium state

σ Surface tension (N·m^{-1})

D_h Hydraulics diameter (m)

j_f Superficial velocity of liquid film (m·s^{-1})

j_g Superficial velocity of vapor core (m·s^{-1})

υ_g Kinetic viscosity of vapor (m·s^{-1})

G Mass flux (kg·m^{-2}·s^{-1})

x Mass quality

α Void fraction

f_i Interfacial frictional coefficient

References

1 Butterwort D, Hewitt G F. Two - phase flow and heat transfer, Oxford University Press, 1977

2 Isbin H S, Vanerwater R, Fauske H K, *et al*. J Heat Transfer, 1961, **83**(5):149-157

3 Hewitt G F, Hall - Taylor N S. Annular two – phase flow, Pergamon Press, New York, 1970

4 Ishii M, Mishima K. Int J Heat Mass Transfer, 1989, **32**(10):1835 - 1846

5 Tomio Okawa, Tsutoshi Kitahara, Kenji Yoshida, *et al*. International Heat and Mass Transfer, 2002, **45**:87 - 98

6 Kataoka I, Ishii M, Nakayama A. Int J Heat Mass Transfer, 2000, **43**:1573 - 1589

7 Paleev I I, Filippovich B S. Int J Heat Mass Transfer, 1966, **9**: 1089 - 1093

8 Henstock W H, Hanratty T J. AICHE, 1976, **22**: 990 - 1000

9 Ren Ling. Experimental research of dryout in vertical upward round tube, Master Thesis, China Institute of Atomic Energy, July 2003